A New Motor Controller for Overloading BLDC-Motors of Low Inductivity, Lightweight and Ready for Admittance and Impedance Model Predictive Control

Manuel Scharffenberg, Fabian Schnekenburger, Michael Wülker, Ulrich Hochberg, Nils-Malte Jahn, Klaus Dorer
Faculty of Mechanical and Process Engineering
University of Applied Sciences Offenburg
Badstr. 24, 77652 Offenburg, Germany
(Manuel.Scharffenberg, Fabian.Schnekenburger, Michael.Wuelker, Ulrich.Hochberg, Nils-Malte.Jahn, Klaus.Dorer)@hs-offenburg.de
https://sweaty.hs-offenburg.de/en

***Abstract*—One of the challenges in humanoid robotics is motion control. Interacting with humans requires impedance control algorithms, as well as tackling the problem of the closed kinematic chains which occur when both feet touch the ground. However, pure impedance control for totally autonomous robots is difficult to realize, as this algorithm needs very precise sensors for force and speed of the actuated parts, as well as very high sampling rates for the controller input signals. Both requirements lead to a complex and heavy weight design, which makes up for heavy machines unusable in RoboCup Soccer competitions.**

A lightweight motor controller was developed that can be used for admittance and impedance control as well as for model predictive control algorithms to further improve the gait of the robot.

I. Introduction

In RoboCup Soccer the objective is to design robots to win a soccer game against the then world champion in 2050 [1]. Actually, the competition is used to teach students, to explore existing technologies, to evaluate new approaches as well as to carry out research work in the field of humanoid robots.

Furthermore, the goal is to design a robot with a human-like gait. This implies the design and use of strong motors, a lightweight and appropriate mechanical design, lightweight sensors and appropriate motor controllers as a precondition for the development and application of sophisticated control strategies. Our work on the first three preconditions was published in earlier workshops [2], [3], [4], in this paper the work on the new motor controller is presented.

The humanoid robot Sweaty, where the new motor controllers are installed, took second place in this year's RoboCup Soccer Adultsize League. It has a height of 172 cm and a weight of 25.6 kg (Fig. 1). Sweaty has 32 degrees of freedom, of which 14 have a strong impact on Sweaty's gait and are equipped with the new motor controllers. The main actuators of the robot Sweaty consist of motor controller, BLDC-motor, gearbox and spindle with ball screw.

Figure 1. Sweaty.

This paper is organized as follows: In Section II the requirements for motor controllers are summarized. In Sub-

section II-A control strategies are shortly described. Subsection II-B focuses on industrial motor controllers which have all the features needed for different control strategies. In Subsection II-C a typical industrial motor controller is described in as much as it is necessary to highlight the differences to Sweaty's motor controllers. Section III describes the hard- and software of the new motor controller. Subsection III-A defines the requirements of the new motor controller; the realized designs of the hard- and software are described in subsection III-B, III-C and III-D. Section IV describes the experiments and the results for the new motor controller, while in section V the future of implementation of wholebody control strategies for Sweaty are addressed.

II. Related Work

A. Whole Body Control Algorithm

Impedance control has been suggested as the strategy employed by the central nervous system [5]. Ivaldi et.al. have recently summarized the approaches for the whole-body control of humanoid robots [6]. Ott, Mukherjee and Nakamura [7] pointed out that there can be stability problems in case of pure impedance control. These stability problems decrease with increasing accuracy of the sensors and decrease with increasing sampling rate. However, in case of totally autonomous systems like those needed in RoboCup soccer, the possibilities of the usage of precise and heavy-weight sensors are limited. Ott showed that in soft environments admittance control with feed forward velocity is superior to impedance control, while in stiff environments impedance control is desirable [7].

It has not yet been decided which type of control will finally be used for Sweaty's whole body motion. It is most likely that both algorithms will have to be used, as the stiffness of the environment changes dramatically during walking: during the swing phase of a foot the environment is not stiff, but as soon as the foot touches the ground the environment suddenly changes.

More complex passivity-based balancing algorithms have been published recently [8]. The new low-level motor controller should also prepare Sweaty's hard- and software for such a type of control.

The underlying hardware controller should be ready to be used for admittance control and impedance control, both including the options of using feed forward control for velocity and force, possibly from a model predictive algorithm.

B. Motor Controller Algorithm

The typical structure of a commercial motor controller is shown in Fig. 2 [9]. Higher-level controls provide information concerning position, speed and force. This information is cascaded as shown in Fig. 2. Position, speed and force are measured and controlled by means of a P, a PI and a second PI controller. Update rates for the controllers should be cascaded: the current controller should be the fastest controller, while the speed controller can be updated with a lower frequency and the position controller with the lowest frequency. For humanoid robots it is essential that the position controller

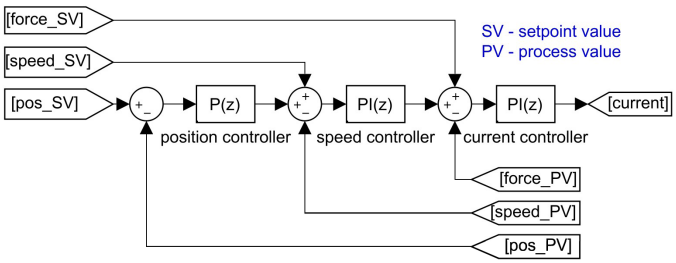

Figure 2. Typical structur of an industrial motor controller [9]

does not have an integral part, as for example in case of a slight misalignment of the feet the controller's signal would increase up to undesired values. By adjusting the parameters of the three internal controllers, this type of motor controller can be programmed for impedance and/or admittance control. It should be emphasized that in case this structure of a controller is used for impedance control, the sampling rates must be very high, as well as the precision of the sensors for speed and force. The sensors must be fast and precise to ensure that the process is stable, especially for humanoid robots, where the environment sometimes changes suddenly form normal to stiff.

C. Motor Controller for BLDC-motors with Low Inductivity

Motor controllers for brushless-DC-motors have been well known and commercialized for decades [10]. A BLDC-motor is characterized by high efficiency and good dynamic behavior. The most efficient and light weight BLDC-motors are iron-free. A consequence of this is that the motor's internal inductivity is very low. To take full advantage of the characteristics of an iron-free BLDC-motor, the hardware of such a motor controller typically has additional inductors to minimize the ripple. A consequence of a high ripple is an increase of switching loss - therefore high ripples are avoided. In contrast to this, for Sweaty some additional losses can be accepted for the sake of the controller's small design and its minimum weight. Therefore no inductors are used. The values provided by Sweaty's high-level control can not be provided with a frequency in the order of magnitude of kHz as it is in industrial applications. In addition an industrial motor controller is not designed to overload a motor far beyond its specifications. The new motor controller is designed to overcome these issues.

III. New Motor Controller

A. Requirement Specification

The new motor controller should be able to overload a BLDC-motor substantially. This feature is of outstanding interest for the usage in the humanoid robot Sweaty, where the motors can be overloaded for a limited time due to the evaporative cooling system of Sweaty's motors. The requirements are summarized in Table I.

It is important that force and speed are independent of the supply voltage. The energy demand of a humanoid robot fluctuates in short periods, as the power which is required for a

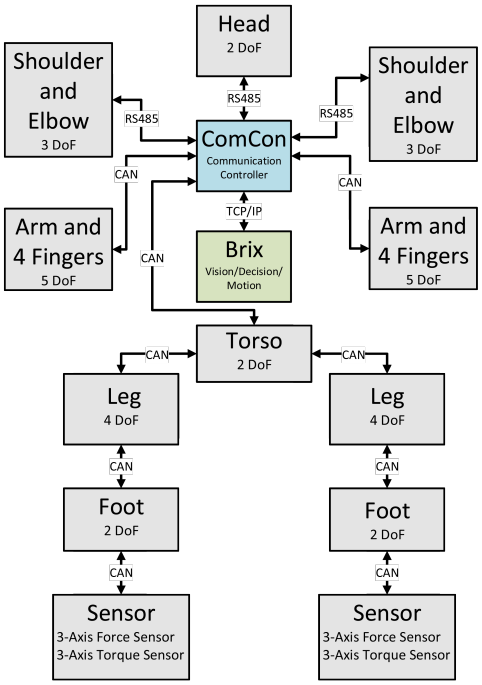

Figure 3. System architecture

Table I
REQUIRED VALUES FOR THE ACTUATOR, CONSISTING OF MOTOR, MOTOR CONTROLLER, GEAR BOX AND SPINDEL WITH BALL SCREW

	Datasheet	short-time values $\leq 2\,\mathrm{s}$	peak-values $\leq 250\,\mathrm{ms}$
Voltage	18 V	29 V	29 V
Speed	$128\,\mathrm{mm\,s^{-1}}$	$160\,\mathrm{mm\,s^{-1}}$	$160\,\mathrm{mm\,s^{-1}}$
Current	5.03 A	16 A	30 A
Force	630 N	2000 N	3800 N
Power	90 W	450 W	870 W

step is not constant over time. Cabling and batteries should not be dimensioned for peak figures of the power consumption, as in this case they would be dramatically oversized for normal operation.

During a fast knee bend, Sweaty's power consumption can vary by more than a factor of ten. Current can even revers and electrical energy is produced which has to be stored in the batteries. In those cases the internal resistance of the battery plays an important role and the voltage drop of the batteries is not negligible. In addition, the supply voltage depends on the SOC (state of charge) of the batteries. In case of the humanoid robot Sweaty, the supply voltage of the motor controller can vary between 22 V and 29 V within 50 ms.

The coil temperature should not influence force and speed of the motor. In peak situations, the coil temperature can increase by 100°C. This has to be taken into account, without compensation the loss of power would be approx. 40 %, just due to the increase of the resistance of the coil.

The underlying control algorithm needs to be programmable for impedance and/or admittance control and for velocity and force feed forward algorithm. No additional sensors should be used. The motor's sensors for commutation must be sufficient to detect speed and position. The force output of the motor should be derived from internal measurements of the motor controller. The sampling rate for the higher-level controls should not be higher than 100 Hz, and a CAN protocol should be used to ensure high reliability and should fit to Sweaty's architecture, see Fig. 3.

Table II
KEY FIGURES OF THE MOTOR

Terminal resistance	$0.323\,\Omega$
Terminal inductance	$0.0283\,\mathrm{mH}$
Torque constant tc	$10.5\,\mathrm{mN\,mA^{-1}}$
Speed constant	$907\,\mathrm{min^{-1}\,V^{-1}}$
Thermal resistance winding-housing	$1.19\,\mathrm{K\,W}$

When reducing speed, the motor controller should convert mechanical to electrical energy and reload the batteries. This is not important for energy recovery, as the amount of recovered energy is almost negligible. It is important to get rid of the mechanical energy and not transform the mechanical energy into heat as it is done in brakes. Parts would heat up and might be destroyed, if the energy released during the slowdown of actuators is transferred into heat.

The motor controller must be light-weight and small, as it needs to be mounted close to the motors to avoid voltage drop in the cables. It should not increase Sweaty's weight substantially (in a final stage, more than 20 motor controllers might be needed). No additional inductance should be installed, the coil inductance must be sufficient.

The controller must fit to a ultra-high efficient and powerful 4pole iron-less BLDC-motor type EC-4pole 22 18V / 323217. The key figures of this motor are given in Tab. II.

B. Hardware Design

The motor controller was designed according to the target specification [11]. It is small and lightweight and consists of two PCBs attached to each other (Fig. 4). The design is straightforward; standard components like inductances were not used. The key component of the power PCB consists of an LTC444 as driver for the three half-bridges. The key component for the low-level controller is a Cortex-M4 (STM32F407VX). A CAN-bus is installed for communication with the server. Power consumption is measured with a shunt. Two temperature measurement devices are installed: one for the housing of the motor and one for the MOSFETs, which are the critical devices concerning overheating. The dimensions are 60 x 34 x 30 mm, the weight is 26 g. The CAN-messages have timestamps which have a correctness better than 20 µs. This was achieved by avoiding any operating system, the code was in written in native C.

C. Sensors

Integral parts of the new motor controller are sensors for the supply voltage U_{suppl} and supply current I_{suppl}, as well as for the temperature of the housing of the motor and the

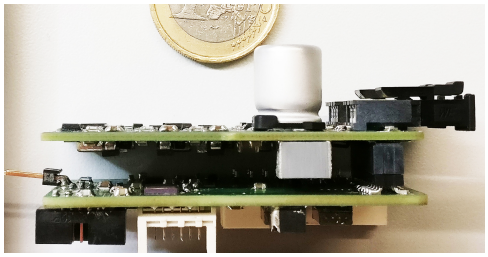

Figure 4. Motorcontroller

temperature of the transistors. Whereas the temperature of the transistors is only used to trigger off an emergency shutdown due to overheating to avoid damage of the system in case of failure, the other measurements are used for control. The internal senors for the magnetic field, which are installed for commutation purpose, are also used for control. In this subsection the equations and the approaches for the use of this sensors are summarized.

The duty cycle of the PWM is denoted D. Neglecting friction and other losses, the force/torque of the motor is related to the current I_{Motor} by the motor's torque constant tc, see Tab. II. Therefore, controlling the duty cycle D of the PWM means controlling the current of the motor and thus force/torque.

The motor current I_{Motor} is linked to the supply voltage U_{suppl}, the resistance of the coil R_{Coil} and the U_{BEMF} according to Eq. (1), wheres as U_{BEMF} can be calculated by dividing the speed of the motor by the motor speed constant from Table II.

$$D = \frac{I_{\mathrm{Motor}} \cdot R_{\mathrm{Coil}} + U_{\mathrm{BEMF}}}{U_{\mathrm{suppl}}} \tag{1}$$

Eq. (1) can be used to calculate D from the required motor current.

The supply voltage of the controller can be measured directly, but R_{Coil} must be derived from other measurements, if the number and size of the sensors are restricted. For speed feed forward control, U_{BEMF} is calculated from the setpoint of the speed.

The resistance of the coil R_{Coil} can be calculated from the temperature of the coil T_{Coil} according to Eq. (2), whereas α_{Cu} is the temperature coefficient of copper. The temperature of the coil can be calculated on the basis of the temperature of the motor's housing and the heat release of the coil [2].

$$R_{\mathrm{Coil}} = R_{\mathrm{Coil},25\,^{\circ}\mathrm{C}} \cdot (1 + (T_{\mathrm{Coil}} - 25\,^{\circ}\mathrm{C}) \cdot \alpha_{\mathrm{Cu}}) \tag{2}$$

To be able to calculate the voltage from the electromagnetic forces U_{BEMF} for feedback control it is essential that the speed of the motor is known precisely. The speed of the motor can be derived from the motor's internal sensors, which sense the magnetic field of the motor and are used for commutation. The alignment of the sensors for the magnetic field are good enough for commutation purpose, but the alignment

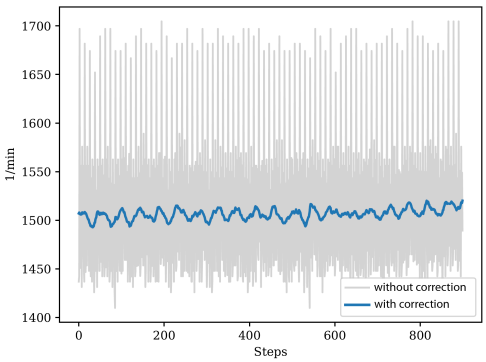

Figure 5. Jitter of the measured speed before and after correction.

is not sufficient for the calculation of the speed. Therefore the following procedure is introduced: After start-up of the system all motors are operated with a constant duty cycle D. The misalignment is measured and the result is stored in the memory of the motor controller. This information is then used to correct the measured motor speed. The difference between the speed which is directly measured and the corrected speed is shown in Fig. 5. The corrected speed is then used to calculate U_{BEMF}.

The process value of the position is measured by the sensors for the magnetic field of the magnets in the motor. As those sensors only provide relative data, it is necessary to calibrate the sensors after each loss of power. Therefore a reference move is programmed after start-up before the controller is put into operation.

The process value of the motor current is needed for feedback control. In principle it can be approximated by dividing the supply current by the duty cycle D (Eq. (3)). However, the sensor for the supply current must be dimensioned for the maximum possible current of 30 A (see Tab. I). The measured figures will be inaccurate for low supply currents and low duty cycles. Therefore, Eq. (1) was rearranged to calculate the process value of the motor current from the actual value of U_{BEMF}, which is derived from the motor speed. Both values were weighted and added in "fuzzy-type" to get reliable figures for the process value of the motor current see Fig. 6.

$$I_{\mathrm{Motor}} = \frac{I_{\mathrm{supply}}}{D} \tag{3}$$

$$I_{\mathrm{Motor}} = \frac{U_{\mathrm{Bus}} \cdot D - U_{\mathrm{BEMF}}}{R_{\mathrm{Coil}}} \tag{4}$$

D. Software Design

1) First approach: In a first step a cascade control structure was evaluated (Fig. 7), which is close to the structure of a well known motor controller [9]. Main difference to a well known motor controller is that both coil temperature and supply voltage are taken into account when calculating the duty cycle. Limiters and algorithm for anti-windup [12] have been included. Another difference is that setpoint values for force and speed are directly used to calculate the duty cycle.

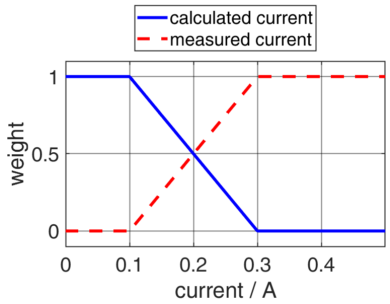

Figure 6. Weighting of the measured (Eq. (3)) and calculated current (Eq. (4)) to get reliable information regarding the motor current.

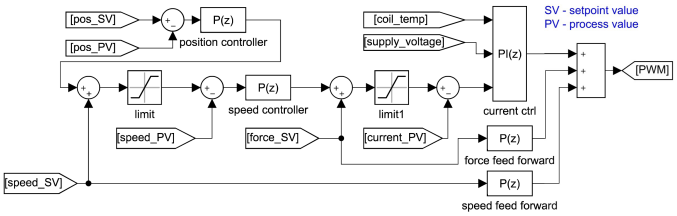

Figure 7. Cascade control structure

The internal frequency of the controllers was 75 kHz, the update rate of the setpoint values was 100 Hz. This controller is superior to a well known controller as it uses setpoint values for speed and force directly to calculate the duty cycle. The controller is fast enough to minimize the impact of fluctuations in coil temperature and supply voltage, but it also gets unstable if the control parameters are chosen for high precision control. In addition, it cannot be programmed for admittance and impedance control independently, as the setpoint value of the position is cascaded down to the underlying controllers.

2) Suggested motor controller: The suggested new motor controller structure is shown in Fig. 8. The current controller, which adjusts the duty cycle, is unmodified. Coil temperature and supply voltage are taken into account when calculating the duty cycle. The setpoint values for speed and force are used directly to calculate the duty cycle. Force, position and speed controllers are acting in parallel. It is possible to choose the controller's parameter in a way so that the control characteristic of the system changes from admittance controlled to impedance controlled. All update rates for the controllers are as fast as possible with Sweaty's architecture: Update rate for the setpoint values is 100 Hz, update rate for the current controller is 75 kHz, as well as for the force controller. The update rate for the position and speed controllers depend on the actual speed of the motor, as the update rate for the process value for those data depend on the motor speed, typical values are 100 Hz to 500 Hz.

IV. Results

A testbench was built for evaluation of the new motor controller (Fig. 9). It consists of a rack and weights well known from a gym. The mass of the weights can be as high as 100 kg. Accelerating sinusoidal to the maximum speed ends

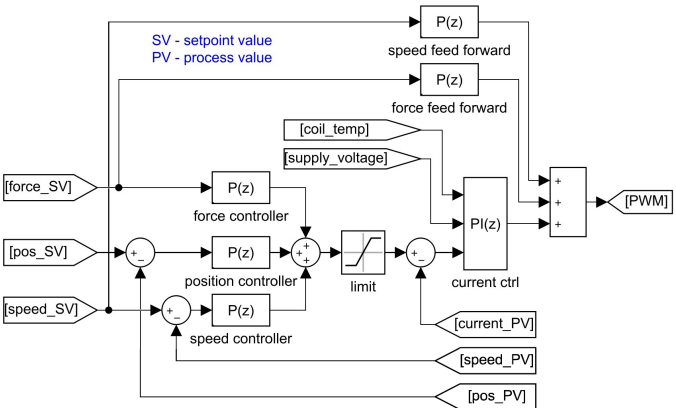

Figure 8. Parallel Control Structure

Figure 9. Testbench

up at an acceleration of $10\,\mathrm{m\,s^{-2}}$, taking the earth gravity into account this is almost the limit of the overloaded actuator. Acceleration, deceleration as well as applying a constant force can be tested. Fig. 10 shows the result of a test with a mass of 65 kg. The mass was moved sinusoidal with a period of 1.2 s. The parameters of the controllers were adjusted in a way that the control loops are stable. A high level controller provided the setpoint values for position, force and speed. It can be seen that the average error in the position finally is as low as 0.22 mm.

Fig. 11 shows the dependency of the position error on the motor temperature and the supply voltage. It can be seen, that a change of the supply voltage is totally compensated, whereas a change of the motor's temperature has a slight impact on the

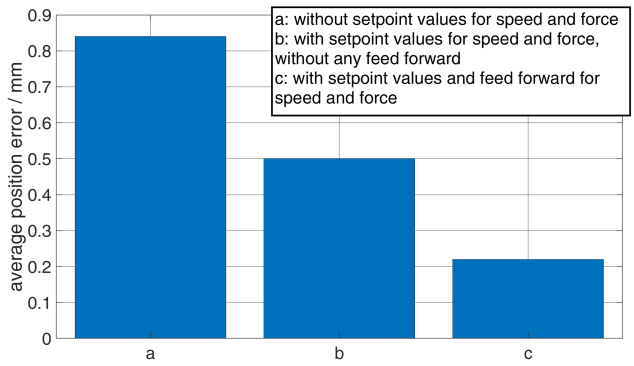

Figure 10. Position Error Results

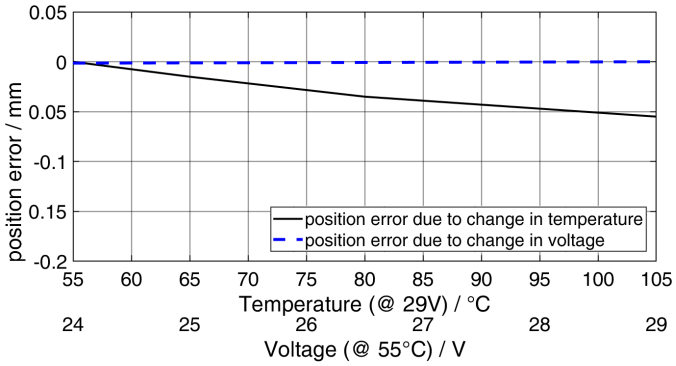

Figure 11. Dependency of the position error on motor temperature and supply voltage

accuracy.

The last Fig. 12 shows that for this test the dimensioning of the actuator is conservative and that the overloading is not a substantial problem, even if the motor's power or the time when the power is needed is beyond the values stipulated in Table I.

The design of the hardware and the code is published under MIT license: https://github.com/SweatyOffenburg/Servo.

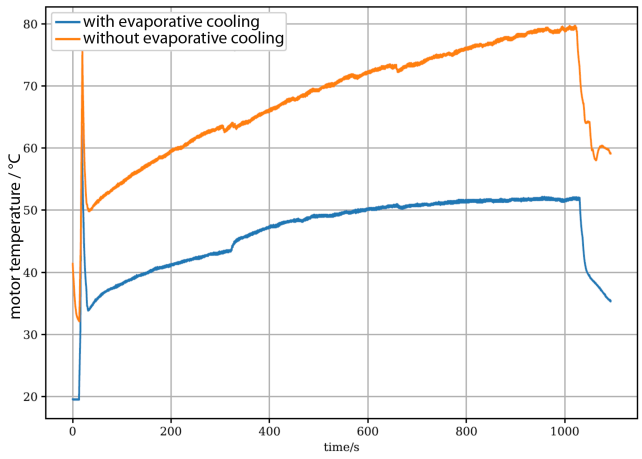

Figure 12. Cooling

V. Conclusion and Future Work

A motor controller has been developed which fits exactly the requirements of the humanoid robot Sweaty. This motor controller is essential for the evaluation of different control strategies of Sweaty's gait. The next steps will be to find out the weak points of Sweaty's mechanical design and to improve those points, before the advantages of the new motor controller can be made use of.

Acknowledgment

The authors would like to thank Hochschule Offenburg for the financial support of the project, as well as maxon motor GmbH, Becker & Müller GmbH and HOBART GmbH for their sponsorship.

References

[1] S. Behnke, M. Schreiber, J. Stuckler, R. Renner, and H. Strasdat, "See, walk, and kick: Humanoid robots start to play soccer," in *Humanoid Robots, 2006 6th IEEE-RAS International Conference on*, 2006, pp. 497–503.

[2] U. Hochberg, A. Dietsche, and K. Dorer, "Evaporative Cooling of Actuators for Humanoid Robots," *Proceedings of the 8th Workshop on Humanoid Soccer Robots, IEEE-RAS International Conference on Humanoid Robots, Atlanta*, November 2013.

[3] M. Scharffenberg, U. Hochberg, K. Dorer, A. Friedrich, and M. Wülker, "Improving Torque and Speed of Joints by Using Rod-and-Lever Systems for Electrically Driven Humanoid Robots," *Proceedings of the 10th Workshop on Humanoid Soccer Robots, IEEE-RAS International Conference on Humanoid Robots, Seoul*, November 2015.

[4] L. Schickl, K. Dorer, M. Wülker, Y. D'Antilio, and U. Hochberg, "Development of a Six-Axis Force and Torque Sensor for the Humanoid Robot Sweaty 2.0," *Proceedings of the 11th Workshop on Humanoid Soccer Robots, IEEE-RAS International Conference on Humanoid Robots, Cancun*, Nov. 2016.

[5] F. Towhidkhah, R. E. Gander, and H. C. Wood, "Model predictive impedance control: A model for joint movement," *Journal of Motor Behavior*, vol. 29, no. 3, pp. 209–222, 1997, pMID: 12453780. [Online]. Available: http://dx.doi.org/10.1080/00222899709600836

[6] S. Ivaldi, J. Babič, M. Mistry, and R. Murphy, "Special issue on whole-body control of contacts and dynamics for humanoid robots," *Autonomous Robots*, vol. 40, no. 3, pp. 425–428, Mar 2016. [Online]. Available: https://doi.org/10.1007/s10514-016-9545-5

[7] C. Ott, R. Mukherjee, and Y. Nakamura, "A hybrid system framework for unified impedance and admittance control," *Journal of Intelligent & Robotic Systems*, vol. 78, no. 3, pp. 359–375, Jun 2015. [Online]. Available: https://doi.org/10.1007/s10846-014-0082-1

[8] B. Henze, M. A. Roa, and C. Ott, "Passivity-based whole-body balancing for torque-controlled humanoid robots in multi-contact scenarios." *International Journal of Robotics Research*, vol. 35, no. 12, p. 1522, 2016. [Online]. Available: http://search.ebscohost.com/login.aspx?direct=true&db=edb&AN=118237390&lang=de&site=eds-live

[9] J. Weidauer, *Elektrische Antriebstechnik: Grundlagen - Auslegung - Anwendungen - Lösungen*. Erlangen: PUBLICIS Corporate Publ., 2008. [Online]. Available: http://swbplus.bsz-bw.de/bsz265396891cov.htm

[10] U. Kafader, *Auslegung von hochpräzisen Kleinstantreiben*. Sachseln: maxon academy, 2006.

[11] F. Schnekenburger, *Entwurf eines Regelkonzepts und Implementierung auf den Aktuatoren des humanoiden Roboters Sweaty: Master-Thesis*, Offenburg, 2016.

[12] T. Buclla, "Servo control of a dc-brush motor," *MICROCHIP Application note AN532*, 2002. [Online]. Available: http://ww1.microchip.com/downloads/cn/AppNotes/cn_00532c.pdf